Article

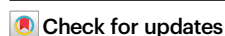# Cathodic oxygen reduction-enabled rhodium-catalyzed (5 + 1) C−H/O−H annulation inspired by fuel cells

Yuan-Qiong Huang[1,2], Li Zhu[1,2] & Tian-Sheng Mei [1] ✉

Transition metal-catalyzed electrochemical C−H annulation with alkynes has emerged as a promising method for constructing heterocycles via formal cycloadditions. However, catalytic electrochemical C−H annulation with alkenes has been less explored. In this study, we report a cathodic oxygen reduction-enabled rhodium catalyzed (5 + 1) annulation reaction between readily available alkenylphenols and alkenes, yielding valuable 2-substituted 2H-chromenes. Unlike existing methods that involve direct oxidation of catalysts at the anode, our protocol uses a sacrificial anode to protect the substrate from overoxidation, while the cathode reduces oxygen, coupling with the Rh[I]. to regenerate the rhodium catalyst. This efficient, atom-economical hetero-cyclization reaction demonstrates a broad scope and functional-group tolerance for diverse biologically relevant molecules, with a Faradaic efficiency greater than 100%.

In recent years, transition metal-catalyzed annulation involving alkynes or alkenes through the activation and cleavage of C−H bonds has emerged as a powerful tool for constructing cyclic scaffolds from acyclic starting materials. This approach offers an alternative to conventional cycloaddition reactions, such as Diels−Alder reactions[1–10]. In this context, catalytic oxidative C−H annulation has garnered significant attention, leading to the development of various annulation methods[11–15]. However, these reactions typically rely on stoichiometric chemical oxidants[16–29]. or internal oxidants to recycle the metal catalyst[30–37]. Recently, synthetic organometallic electrochemistry has experienced a resurgence,[38–45]. where transition-metal catalysts control reaction selectivity and electrodes manage redox chemistry[46–54]. In this field, transition metal-catalyzed electrochemical C−H functionalization[55–59]. has emerged as a promising approach for constructing heterocycles through formal (n + m)[60–75]. cycloadditions, with significant contributions from research teams led by Ackermann, Lei, Mei, and Xu, among others. For example, Ackerman et al. provided an early example of Rh-catalyzed electrochemical C−H annulation of benzoic acids or benzamides with acrylates and 2-alkenylphenols with alkynes to synthesize five- or seven-membered cyclic compounds[62]. Mechanistic studies indicated that rhodium(I) was oxidized to

rhodium(III) species by anodic oxidation to complete the catalytic cycle[74]. Our research team has developed catalytic electrochemical vinylic C−H annulation with alkynes for synthesizing cyclic compounds using iridium[69]. or rhodium catalysis[72]. All reactions involved electrochemical direct oxidation of the metal catalyst to complete the catalytic cycle. However, reports on electrochemical metal-catalyzed reactions involving oxygen are scarce. Recently, Stahl[76,77]. reported the use of a manganese-tetraphenylporphyrin catalyst that couples electrochemical oxygen reduction and water oxidation to facilitate substrate oxidant reactions. In this reaction, manganese porphyrins as mediators to generate a $Mn^V = O$ species that promotes oxygen-atom-transfer (OAT) to the organic substrate.

Molecular oxygen ($O_2$), as a green chemical oxidant, is widely used in both homogeneous and heterogeneous catalysis[78,79]. $O_2$ activation and its reaction with organic molecules generally occur through three mechanisms[80–82]. (1) In the first mechanism, $O_2$ can accept a single electron to generate reactive oxygen species (ROS), which then trigger radical chain reaction (Fig. 1A left). (2) In the second mechanism, a typical example is cytochrome P450, where reductive activation of $O_2$ generates metal-oxo species, leading to an OAT reaction (Fig. 1A, middle). This type of reaction,

[1]State Key Laboratory of Organometallic Chemistry, Shanghai Institute of Organic Chemistry, University of Chinese Academy of Sciences, CAS, Shanghai, China. [2]These authors contributed equally: Yuan-Qiong Huang, Li Zhu. ✉e-mail: mei7900@sioc.ac.cn
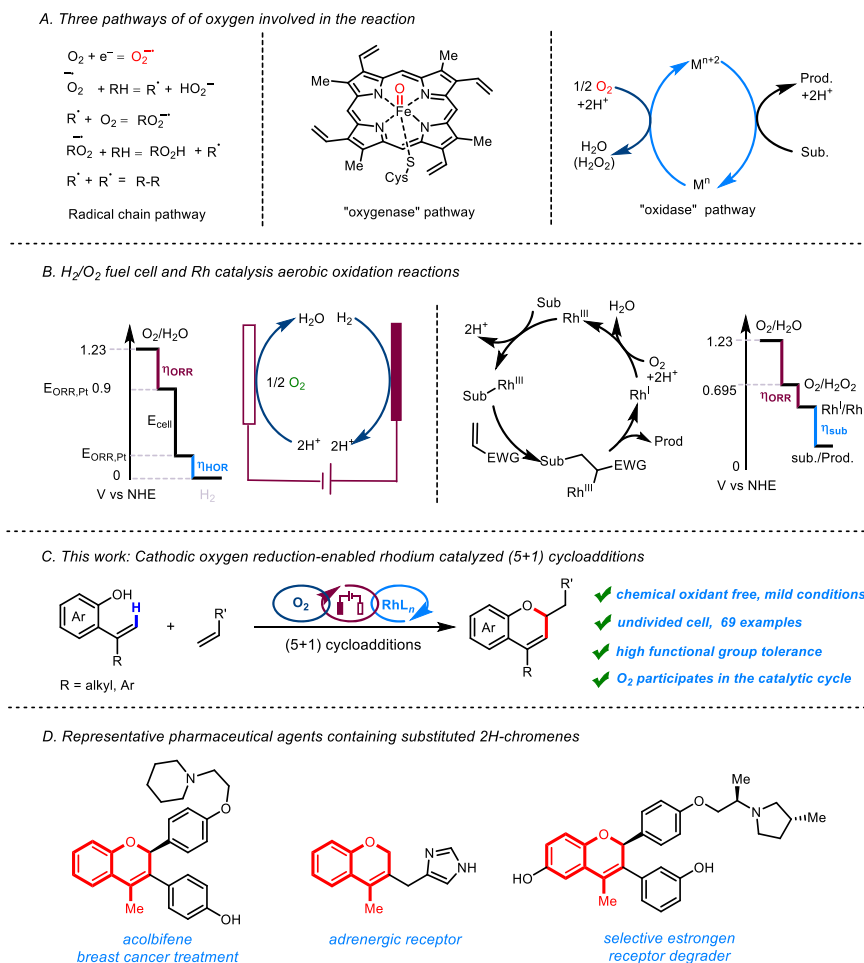
**Fig. 1 | Enantioselective electrochemical reductive cross-couplings. A** Three pathways of oxygen involved in the reaction. **B** $H_2/O_2$ fuel cell and Rh catalysis aerobic oxidation reactions. **C** This work: Cathodic oxygen reduction-enabled rhodium catalyzed (5 + 1) cycloadditions. **D** Representative pharmaceutical agents containing substituted 2H-chromenes.

also known as an "oxygenase" reaction, requires a sacrificial reductant. (3) The third mechanism involves a four-electron process in the $O_2$ reduction reaction (ORR). Here, $O_2$ reduction coupled with metal catalysis produces hypervalent state metal species that oxidize the substrate without an oxygen-atom transfer process (Fig. 1A, right). This type of reaction is known as an "oxidase" reaction, where the reduction of $O_2$ and substrate oxidation occur independently.

Electrochemical processes in fuel cells involve reactions where $O_2$ reacts with protons and electrons to produce water. These reactions require an "overpotential" ($\eta_{ORR}$) to overcome kinetic barriers, calculated as $\eta_{ORR} = E^{\circ}_{O2/H2O}$ (1.23 V vs NHE) $- E^{\circ}_{ORR,Pt}$ (0.9 V vs NHE). The overpotentials for hydrogen oxidation ($\eta_{HOR} = E^{\circ}_{H+/H2} - E^{\circ}_{HOR,Pt}$) is lower, So improving fuel cell efficiency involves reducing both $\eta_{ORR}$ and $\eta_{HOR}$ (Fig. 1B, left). Inspired by Stahl's aerobic oxidation reactions and the concept of overpotential in fuel cells, we propose a reaction initiated by C−H activation of substrates (Sub) to generate a "Sub−Rh" intermediate (Fig. 1B, right). This intermediate undergoes regioselective alkene migratory insertion into the Rh−C bond, followed by β-H elimination to afford a C−H bond alkenylation product and $Rh^I$. $Rh^I$ can be oxidized by $H_2O_2$, regenerated from $O_2$ reduction, to produce $Rh^{III}$ and $H_2O$. With the potentials of the $O_2/H_2O_2 = 0.695$ V vs SHE, $O_2/H_2O = 1.23$ V vs SHE, $H_2O_2/H_2O = 1.76$ V vs SHE, $Rh^I/Rh^{III} \approx 0.44$ V vs SCE,[61] $Rh^I/Rh^{III}$. potential is close to the $O_2/H_2O_2$ potential, indicating a small overpotential for $O_2$ reduction. In this reaction, no OAT occurs (which is different from Stahl's aerobic oxidation reactions), requiring

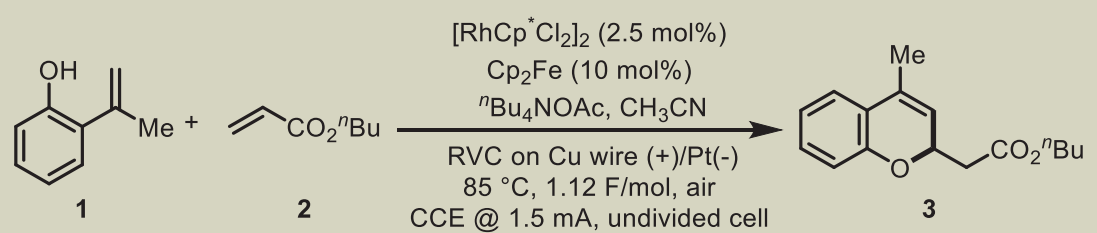a sacrificial reductant and utilizing electrochemical energy to overcome kinetic barriers.

Herein, we present an electrochemical oxygen reduction-enabled rhodium-catalyzed C−H annulation of 2-alkenylphenols with alkenes, leading to the synthesis of 2H-chromene skeleton. This method offers an approach to constructing six-membered heterocycles through formal (5 + 1) cycloadditions (Fig. 1C). In addition, the 2H-chromene skeleton, especially those substituted at the C2 position, has attracted considerable attention as a crucial structural motif in the discovery of new drug candidates (Fig. 1D)[83–86].

## Results
### Optimization studies
The optimization of reaction conditions began with using 2-(prop-1-en-2-yl)phenol (**1**) and commercially available butyl acrylate (**2**) as olefin-coupling partners in an undivided cell. Reticulated vitreous carbon (RVC) and platinum (Pt) plates were used as anode and cathode materials, respectively (Table 1). The reactions were performed with 2.5 mol% [Cp*RhCl$_2$]$_2$, 2.0 equivalents of $^nBu_4NOAc$, and heating a mixture of acrylate with 2.0 equivalents of phenol derivatives in $CH_3CN$ at 85 °C. After 4 h of electrolysis under a constant current of 1.5 mA, the main product **3** was obtained in 56% yield (entry 4). Product **3** was identified as a 2H chromene structure with a six-membered ring after (5 + 1) cyclization. The yield increased to 84% with the addition of 0.1 equivalent of ferrocene as an electrochemical mediator[87]. (entry 1). The reaction did not proceed with other anion quaternary ammonium

**Table 1 | Optimization of reaction conditions[a]**



| Entry | Deviation from Standard Conditions | 3 Yield (%)[b] |
|---|---|---|
| 1 | none | 84 |
| 2 | $^nBu_4NPF_6$ or $^nBu_4NBF_4$ instead of $^nBu_4NOAc$ | trace |
| 3 | $CH_3OH$ instead of $CH_3CN$ | trace |
| 4 | no $Cp_2Fe$ | 56 |
| 5 | Pt instead of RVC | nr |
| 6 | 75 °C | 65 |
| 7 | 65 °C | 63 |
| 8 | [Cp*IrCl$_2$]$_2$ instead of [Cp*RhCl$_2$]$_2$ | trace |
| 9 | [(p-cymene)RuCl$_2$]$_2$ instead of [Cp*RhCl$_2$]$_2$ | trace |

[a] Reaction conditions: **1a** (0.4 mmol), **2a** (0.2 mmol), [Cp*RhCl$_2$]$_2$ (2.5 mol%), $^nBu_4NOAc$ (2.0 equiv), $Cp_2Fe$ (10 mol%), MeCN (4 mL) in undivided cell, I = 1.5 mA, 4 h. $^nBu$ = normal butyl group [b] Isolated yield.

salts, such as $^nBu_4NPF_6$ or $^nBu_4NBF_4$, used as the electrolyte (entry 2). The target product was also not obtained when MeOH was used instead of MeCN as the solvent (entry 3). Using Pt instead of RVC as the anode completely suppressed the reaction (entry 5). Reducing the temperature to 75 °C or 65 °C resulted in lower yields of 65% and 63%, respectively (entries 6 and 7). Other catalysts, such as [RuCl$_2$(p-cymene)$_2$] or [IrCp*Cl$_2$]$_2$, were ineffective (entries 8 and 9).

## Substrate scope

With the optimized conditions established, we investigated the substrate scope of the reaction. As shown in Fig. 2, the reaction conditions are compatible with acrylates bearing a range of functional groups. Acrylate substrates with either electron-withdrawing or electron-donating substituents produced the corresponding 2H chromene products in moderate to good yields. For instance, alkyl acrylates—whether primary, secondary, or tertiary, including ethyl (Et), n-butyl (nBu), benzyl (Bn), cyclopentyl, cyclohexyl, tert-butyl (tBu), and adamantyl—were well-tolerated and afforded products in moderate to good yields (**3–11**, 56–86%). An aryl acrylate was also compatible, yielding compound **12** at 80%. In addition, acrylates featuring a poly-PEG motif could be coupled with reagent **1**. Even ethylene glycol acrylates with unprotected hydroxyl groups were well-tolerated, providing yields between 73% and 80% (**13–16**). The annulation with perfluoro acrylates (**17** and **18**) demonstrated high efficiency, achieving yields of 80–81%. Various alkyl primary and secondary acrylates with reductively labile functionalities, including phthalimide (**19**), ester (**20**), NBoc (**21**), ketone (**22**), and ketal (**23**), were effectively accommodated. Additionally, groups prone to oxidative degradation, such as olefin (**24**), and heterocycles like furan (**25**) and thiophene (**26**), were examined, yielding the desired products in good yields (80–81%). A series of medicinally relevant oxacyclic rings were obtained with high yields (**27–29**, 71–75%). Other electron-withdrawing alkenes, such as vinyl sulfone, acrylamide, and acrylonitrile, also participated as olefin-coupling partners, achieving yields between 66% and 77% (**30–32**).

Butyl acrylate was chosen as the alkene partner to further investigate the substrate scope of 2-alkenylphenols. Aryl C–X bonds (X = F,

Cl, Br) with various positions on aromatic ring, which are labile to reductive conditions, were compatible with this reaction (**33–35, 39–41**). Electron-withdrawing groups, such as CF$_3$ and ester, facilitated the formation of the desired annulation products in synthetically useful yields (**37–38**, 60–64%). Bi-substituted 2-vinylphenols coupled with butyl acrylate yielded the desired product **42** at 76% yield. When the methyl group at the 2-position of the alkenyl substituent on the benzene ring were replaced by a more hindered phenyl group, the yield decreased, with product **43** obtained at a yield of 43%. Both electron-deficient and electron-rich groups in the *para* position of the benzene ring afforded the products (**44–49**) in 39 – 60% yields. The reaction tolerates different substituents in the 2-position of alkenyl, such as methyl or phenyl groups, but also tolerates other substituents, such as trifluoromethyl (**50**), hydrogen (**51**), or ethyl (**52**).

This reaction was also compatible with acrylates derived from alcohols with complex structures found in some natural products and drugs, resulting in the formation of a 2H chromene structure. The system effectively accommodated natural chiral alcohols containing terpene structures corresponding to acrylates, yielding the desired products (Fig. 3). These included: primary alcohols such as (S)-(−)-perillyl alcohol (**53**, 80%), (S)-(−)-β-citronellol (**54**, 70%), and phytol (**55**, 78%); secondary alcohols like (−)-isopulegol (**56**, 61%), (+)-menthol (**57**, 73%), pregnenolone (**58**, 72%), dehydroepiandrosterone (**59**, 72%), cholesterol (**60**, 73%), and estradiol (**61**, 60%); and tertiary alcohols such as cedrol (**62**, 60%). The desired annulation products were obtained using α-amino acids or chiral alcohol as reaction partners (**63–64**, 60–83%). Glycoside compounds, which have significant applications biochemistry and pharmaceutical chemistry, were also efficiently reacted to produce product **65–67** (79–83%)[88,89]. Estrone acrylate was well tolerated, yielding 88% (**68**). In addition, a series of inhibitors, including icaridin (**69**, 70% yield), idebenone (**70**, 70% yield), and ezetimibe (**71**, 66% yield), reacted with 2-alkenylphenols **1** to give the desired products in moderate yields.

## Discussion

To gain further insight into the reaction mechanism, we conducted a series of experiments. Control experiments replacing $Cp_2Fe$ with $Fc^+PF_6^-$ in the absence of electricity did not yield the desired product
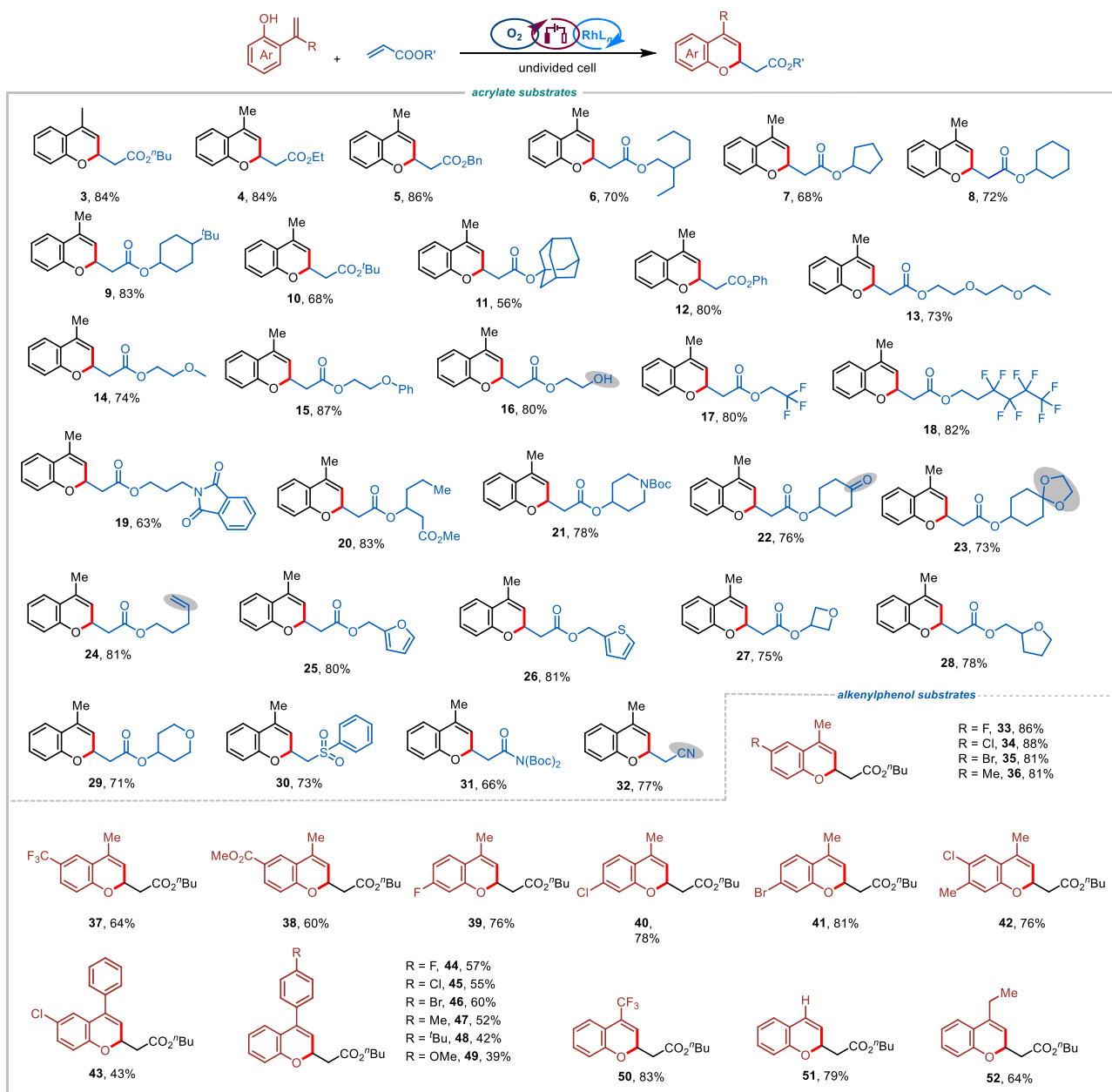
**Fig. 2 | Scope of (5 + 1) annulation cyclic alcohols.** [a]Reaction conditions: 2-alkenylphenols (0.4 mmol), acrylate (0.2 mmol), [n]Bu$_4$NOAc (0.4 mmol), Cp$_2$Fe (10 mol %), [RhCp*Cl$_2$]$_2$ (2.5 mol%), and MeCN (4 mL) in an undivided cell with RVC (2.0 × 8.0 × 30 mm) as the anode and Pt (10 × 10 mm) as the cathode at 85 °C and 1.5 mA for 4 h. [b]Yield of isolated product based on acrylate.

**3** (Fig. 4A). According to work by Sevov,[90]. Cp$_2$Fe serves multiple roles: (i) it rapidly oxidizing low-valency Cu intermediates to prevent Cu precipitation on the cathode (where the anode, RVC, is attached to Cu wire, which may undergo electrolysis during the reaction) and (ii) it providing anodic overcharge protection to prevent substrate oxidation. Without electricity, using a rhodium catalyst (25 mol%) in air resulted in a 25% yield of the desired product **3**. In an N$_2$ atmosphere, the yield dropped to 15%, suggesting that O$_2$ did not facilitate efficient catalyst turnover and that Rh[III]. reductive elimination produced Rh[I]. rather than Rh[III+n]. reductive elimination (Fig. 4B).

Under standard conditions, replacing RVC with Fe as the anode in air yielded products **3** at 68%. The yield of product **3** was only 7% when the experiment was carried out in a nitrogen atmosphere. This indicates that the reaction could also be cycled without the action of anodic oxidation. Using Pt as the anode and employing Et$_3$N

sacrificial agents increased the yield to 21%. Omitting Et$_3$N results in the reaction not proceeding (Fig. 4C), indicated that the anode needed sacrificial agents, and oxygen was reduced at the cathode. Interestingly, using RVC and Pt wire in air improved the yield of products **3** to 38%. In an N$_2$ atmosphere, the yield was 18%, indicating that Rh[I]. might be oxidized on the RVC electrode. In a divided cell, placing rhodium in the anodic cell gave products **3** with a 12% yield, while placing rhodium in the cathodic cell resulted in a 30% yield. This indicates that Rh[I]. could be oxidized by the superoxide anion generated at the cathode by reducing oxygen, and direct oxidation of Rh[I]. on the anode is also possible (Fig. 4D). The Faradaic efficiency in the reaction was about 150%, which also proved that in addition to the anodic oxidation process, there was also the participation of oxygen at the cathode, making the Faradaic efficiency exceed 100%. A sacrificial Fe anode was as effective as RVC. Treating **1** with **2a** gave
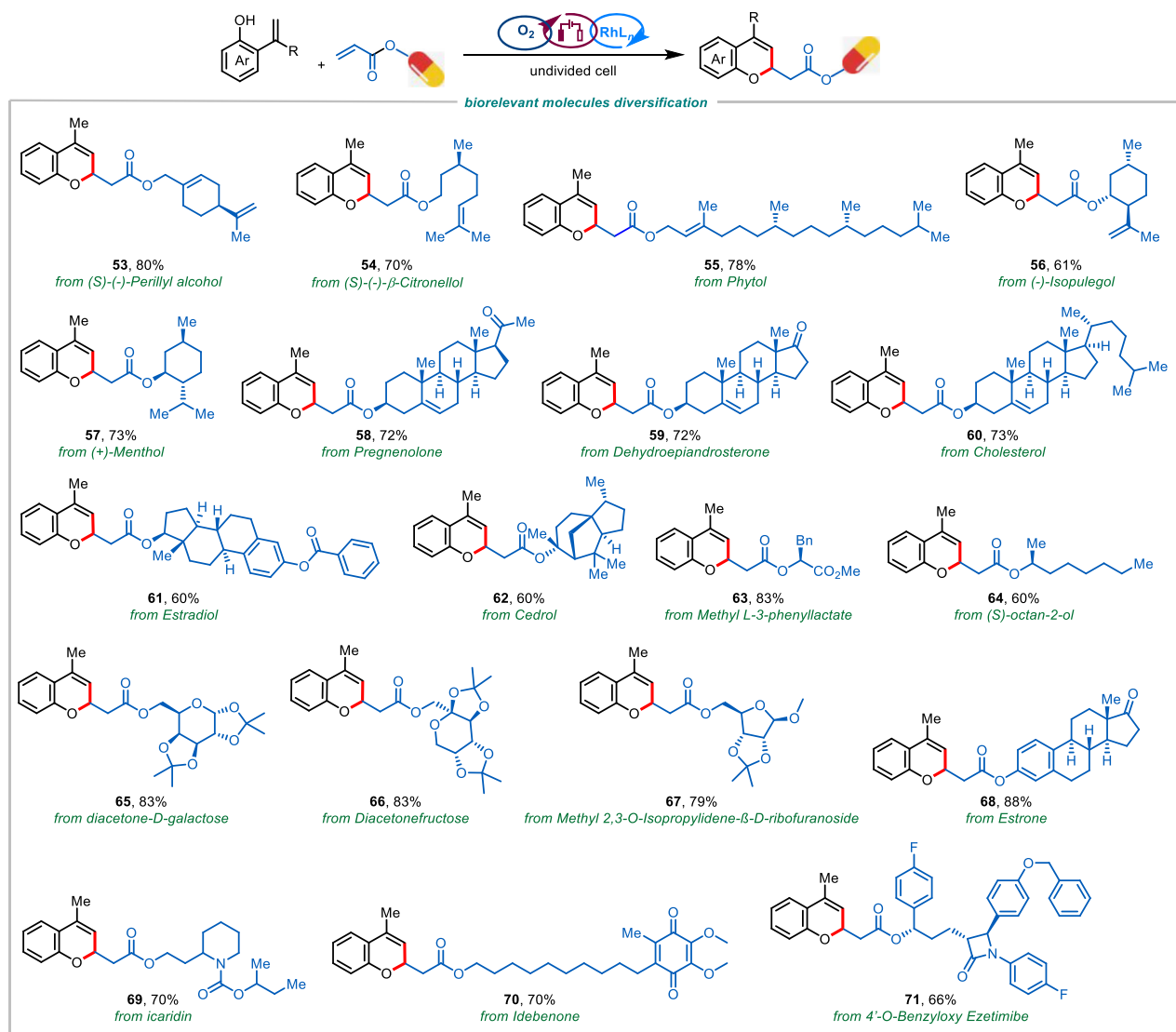
**Fig. 3 | Biorelevant molecules diversification of acrylate.** [a]Reaction conditions: **1** (0.4 mmol), acrylate (0.2 mmol), $^nBu_4NOAc$ (0.4 mmol), Cp₂Fe (10 mol%), [RhCp*Cl₂]₂ (2.5 mol%), and MeCN (4 mL) in an undivided cell with RVC (2.0 × 8.0 × 30 mm) as the anode and Pt (10 × 10 mm) as the cathode at 85 °C and 1.5 mA for 4 h. [b]Yield of isolated product based on acrylate.

product **4** at 67%. Using Cu instead of RVC as the anode increased the yield of product **4** to 76%. Other substrates using Fe or Cu as the anode showed similar results (Fig. 4E). The reaction was inhibited by the addition of 5,5-dimethyl-1-pyrroline N-oxide (DMPO), supporting the presence of a radical intermediate (Fig. 4F). We also performed a series of cyclic voltammetry studies of [RhCp*Cl₂]₂, reactants **1** and **2**, and product **3** at ambient temperature (Fig. 4G). We observed irreversible oxidation of [RhCp*Cl₂]₂ at 1.40 and 1.71 V *versus* AgNO₃/Ag, whereas Cp₂Fe exhibited oxidation peaks at 0.1 V *versus* AgNO₃/Ag. Reactants **1** and **2** did no shown any significant oxidation peaks, but product **3** had oxidation peaks at 1.32 V *versus* AgNO₃/Ag. Thus, Cp₂Fe was excluded as an oxidation medium. Giving the oxidation peak potential of [RhCp*Cl₂]₂, Rh[III]. could not be further oxidized to a higher valence state using Fe or Cu as the anode. Therefore, an oxidation-induced reductive elimination process was ruled out, and it seems plausible that Rh[III]. underwent reductive elimination to give Rh[I]. A three-electrode system was used, and a voltmeter was used to measure the anode potential of the reaction relative to the reference electrode during the standard process (Fig. 4H). After the reaction started, the potential of the anode relative to the AgNO₃/Ag

reference electrode gradually dropped to −0.2 V, and then stabilized between −0.2 and −0.3 V during the process, which also confirmed that the lower oxidation potential in the reaction system can prevent excessive oxidation of the substrate. In an air environment, oxygen would be an ideal electron acceptor and an effective oxidizing agent for Rh[I]. To gain further insight into this electrochemical rhodium-catalyzed annulation system, initial rates were measured for substrates with electronically varied substituents on the alkene aromatic ring, and faster rates were observed with substrates bearing electron-withdrawing groups. A Hammett plot using σ para parameters reveals a positive slope ($\rho = 0.20$; Fig. 4I).

Based on our mechanistic studies and literature reports, a plausible catalytic cycle is illustated in Fig. 5. Initially, C − H/O − H activation forms rhodacycle **A**. Alkene **2** then coordinates and undergoes regioselective migratory insertion into the Rh−C bond to generate the eight-membered rhodacycle intermediate **B**. Instead of undergoing reductive elimination, this intermediate evolves through β-hydride elimination to give the conjugated system **C**, which then undergoes reductive elimination to form the Rh[I]. complex **E**. Complex **C** then undergoes Michael addition to deliver the desired product **3**. The cathode reduces
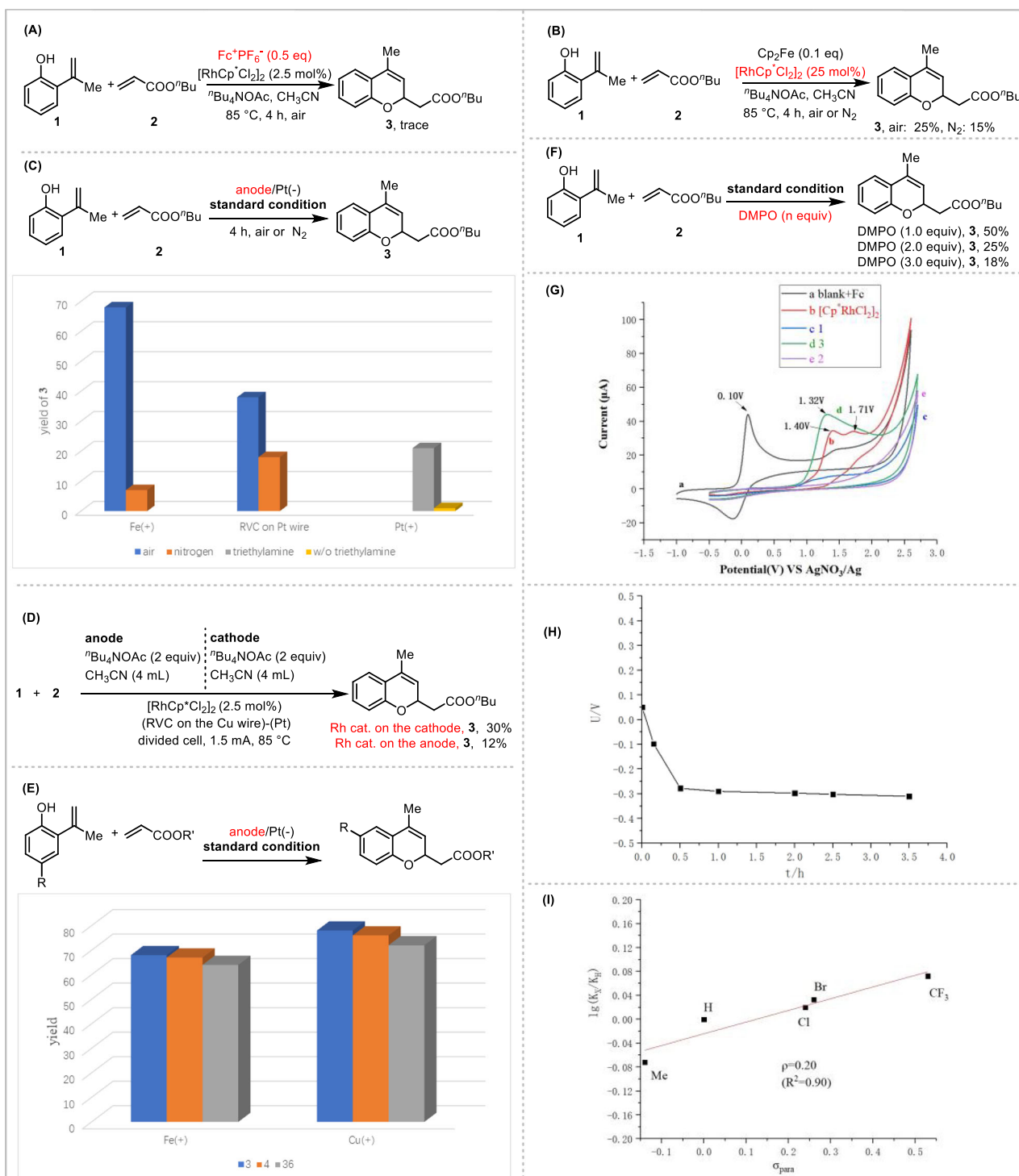
**Fig. 4 | Mechanistic investigation. A–F** Control experiments. **G** Cyclic voltammetry. **H** Anode potential of the reaction. **I** Hammett plot of relative initial rates.

oxygen, which, in conjuction with the Rh$^I$. complex **E**, generate Rh$^{III}$. to complete the catalytic cycle[16].

In summary, we demonstrated an example of cathodic reductive oxygen-enabled rhodium-catalyzed (5 + 1) cyclizations to synthesize 2-substituted 2H-chromenes. This method is compatible with acrylates and alcohols with complex structures found in some natural products and drugs. Preliminary mechanistic experiments indicate that the cathode reduces oxygen in conjunction with Rh$^I$. to regenerate rhodium catalysis. Our research group is continuing to develop the cathodic reduction-enabled transition-metal catalytic method.

## Methods

### General procedure for the electrolysis

The electrocatalysis was equipped with RVC ($0.2 \times 0.8 \times 3.0$ cm$^3$) as anode and Pt as cathode ($1.0 \times 1.0$ cm$^2$). 2-Alkenylphenols **1a** (2.0 equiv), ethyl acrylate **2a** (0.2 mmol, 1.0 equiv), $^n$Bu$_4$NOAc (0.4 mmol, 2.0 equiv), [Cp*RhCl$_2$]$_2$ (2.5 mol%), Fc (10 mol%) were dissolved in MeCN (4.0 mL). Electrocatalysis was performed at 85 °C with a constant current of 1.5 mA maintained for 4 h. After the reaction, the reaction mixture was concentrated in vacuo. The resulting residue was purified by silica gel flash chromatography to give the product **3**.
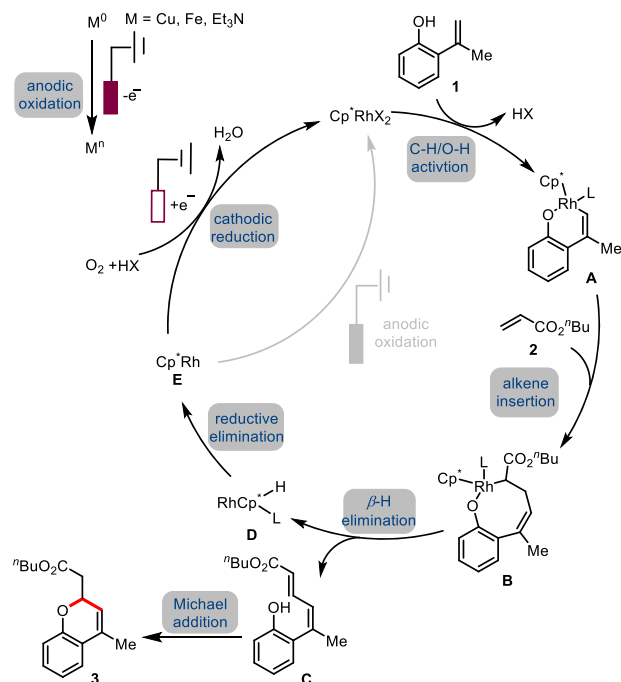
**Fig. 5 | Proposed catalytic cycles.** Proposed Rh-catalyzed (5 + 1) C–H/O–H Annulation mechanism.

More experimental procedures and a photographic guide for rhodium-catalyzed (5 + 1) annulation are provided in the Supplementary Information.

## Data availability

The data supporting the findings of this study are available within the article and its Supplementary Information files. Data is available from the corresponding authors upon request.

## References

1. Docherty, J. H. et al. Transition-metal-catalyzed C–H bond activation for the formation of C–C bonds in complex molecules. *Chem. Rev.* **123**, 7692–7760 (2023).
2. Mandal, D., Roychowdhury, S., Biswas, J. P., Maiti, S. & Maiti, D. Transition-metal-catalyzed C–H bond alkylation using olefins: recent advances and mechanistic aspects. *Chem. Soc. Rev.* **51**, 7358–7426 (2022).
3. Zhang et al. Recent advances in chelation-assisted site- and stereoselective alkenyl C–H functionalization. *Chem. Soc. Rev.* **50**, 3263–3314 (2021).
4. Dalton, T., Faber, T. & Glorius, F. C. – H Activation: Toward Sustainability and Applications. *ACS Cent. Sci.* **7**, 245–2261 (2021).
5. Rej, S., Ano, Y. & Chatani, N. Bidentate directing groups: An efficient Tool in C–H bond functionalization chemistry for the expedient construction of C–C bonds. *Chem. Rev.* **120**, 1788–1887 (2020).
6. Park, Y., Kim, Y. & Chang, S. Transition metal-catalyzed C–H amination: Scope, mechanism, and applications. *Chem. Rev.* **117**, 9247–99301 (2017).
7. Gulías, M. & Mascareñas, J. L. Metal-catalyzed annulations through activation and cleavage of C–H bonds. *Angew. Chem. Int. Ed.* **55**, 11000–11019 (2016).
8. Ackermann, L. Carboxylate-assisted ruthenium-catalyzed alkyne annulations by C–H/Het–H bond functionalizations. *Acc. Chem. Res.* **47**, 281–295 (2014).
9. Engle, K. M., Mei, T. S., Wasa, M. & Yu, J. Q. Weak coordination as a powerful means for developing broadly useful C–H functionalization reactions. *Acc. Chem. Res.* **45**, 788–802 (2012).
10. Colby, D. A., Bergman, R. G. & Ellman, J. A. Rhodium-catalyzed C–C bond formation via heteroatom-directed C–H bond activation. *Chem. Rev.* **110**, 624–655 (2010).
11. Liu, C. X. et al. Rhodium-catalyzed asymmetric C–H functionalization reactions. *Chem. Rev.* **123**, 10079–100134 (2023).
12. Davison, R. T., Kuker, E. L. & Dong, V. M. Teaching aldehydes new tricks using rhodium- and cobalt-hydride catalysis. *Acc. Chem. Res.* **54**, 1236–1250 (2021).
13. Piou, T. & Rovis, T. Electronic and steric tuning of a prototypical piano stool complex: Rh(III) catalysis for C–H functionalization. *Acc. Chem. Res.* **51**, 178–1180 (2018).
14. Song, G. Y., Wang, F. & Li, X. W. C–C, C–O and C–N bond formation via rhodium(iii)-catalyzed oxidative C–H activation. *Chem. Soc. Rev.* **41**, 3651–3678 (2012).
15. Satoh, T. & Miura, M. Oxidative coupling of aromatic substrates with alkynes and alkenes under rhodium catalysis. *Chem. Eur. J.* **16**, 11212–11222 (2010).
16. Stuart, D. R., Bertrand-Laperle, M., Burgess, K. M. N. & Fagnou, K. Indole synthesis via rhodium catalyzed oxidative coupling of acetanilides and internal alkynes. *J. Am. Chem. Soc.* **130**, 16474–16475 (2008).
17. Rakshit, S., Patureau, F. W. & Glorius, F. Pyrrole synthesis via allylic sp³. C–H activation of enamines followed by intermolecular coupling with unactivated alkynes. *J. Am. Chem. Soc.* **132**, 9585–9587 (2010).
18. Chidipudi, S. R., Khan, I. & Lam, H. W. Functionalization of $C_{sp3-H}$ and $C_{sp2-H}$ bonds: Synthesis of spiroindenes by enolate-directed ruthenium-catalyzed oxidative annulation of alkynes with 2-Aryl-1,3-dicarbonyl compounds. *Angew. Chem. Int. Ed.* **51**, 12115–12119 (2012).
19. Nan, J. et al. Ru^II-Catalyzed vinylative dearomatization of naphthols via a C(sp²)–H bond activation approach. *J. Am. Chem. Soc.* **135**, 17306–17309 (2013).
20. Seoane, A., Casanova, N., Quiñones, N., Mascareñas, J. L. & Gulías, M. Rhodium(III)-catalyzed dearomatizing (3 + 2) annulation of 2-alkenylphenols and alkynes. *J. Am. Chem. Soc.* **136**, 7607–7610 (2014).
21. Zheng, J., Wang, S. B., Zheng, C. & You, S. L. Asymmetric dearomatization of naphthols via a Rh-catalyzed C(sp²)–H functionalization/annulation reaction. *J. Am. Chem. Soc.* **137**, 4880–4883 (2015).
22. Ueura, K., Satoh, T. & Miura, M. An efficient waste-free oxidative coupling via regioselective C–H bond cleavage: Rh/Cu-catalyzed reaction of benzoic acids with alkynes and acrylates under air. *Org. Lett.* **9**, 1407–1409 (2007).
23. Hyster, T. K. & Rovis, T. Rhodium-catalyzed oxidative cycloaddition of benzamides and alkynes via C–H/N–H activation. *J. Am. Chem. Soc.* **132**, 10565–10569 (2010).
24. Pham, M. V., Ye, B. H. & Cramer, N. Access to sultams by rhodium(III)-catalyzed directed C–H activation. *Angew. Chem. Int. Ed.* **51**, 10610–10614 (2012).
25. Dong, W. R., Wang, L., Parthasarathy, K., Pan, F. F. & Bolm, C. Rhodium-catalyzed oxidative annulation of sulfoximines and alkynes as an approach to 1,2-benzothiazines. *Angew. Chem. Int. Ed.* **52**, 11573–11576 (2013).
26. Quiñones, N., Seoane, A., García-Fandiño, R., Mascareñas, J. L. & Gulías, M. Rhodium(III)-catalyzed intramolecular annulations involving amide-directed C–H activations: synthetic scope and mechanistic studies. *Chem. Sci.* **4**, 2874–2879 (2013).
27. Seoane, A. et al. Rhodium-catalyzed annulation of ortho-alkenyl anilides with alkynes: Formation of unexpected naphthalene adducts. *Angew. Chem. Int. Ed.* **58**, 1700–1704 (2019).
28. Seoane, A., Casanova, N., Quinones, N., Mascarenas, J. L. & Gulias, M. Straightforward assembly of benzoxepines by means of a

rhodium(III)-Catalyzed C–H functionalization of o-Vinylphenols. *J. Am. Chem. Soc.* **136**, 834–837 (2014).

29. Casanova, N., Seoane, A., Mascareñas, J. L. & Gulías, M. Rhodium-catalyzed (5+1) annulations between 2-alkenylphenols and allenes: A practical entry to 2,2-disubstituted 2H-chromenes. *Angew. Chem. Int. Ed.* **54**, 2374–2377 (2015).

30. Hyster, T. K., Knoerr, L., Ward, T. R. & Rovis, T. Biotinylated Rh(III) complexes in engineered streptavidin for accelerated asymmetric C–H activation. *Science* **338**, 500–503 (2012).

31. Ye, B. H. & Cramer, N. Chiral cyclopentadienyl ligands as stereo-controlling element in asymmetric C–H functionalization. *Science* **338**, 504–506 (2012).

32. Huckins, J. R., Bercot, E. A., Thiel, O. R., Hwang, T. L. & Bio, M. M. Rh(III)-Catalyzed C–H activation and double directing group strategy for the regioselective synthesis of naphthyridinones. *J. Am. Chem. Soc.* **135**, 14492–14495 (2013).

33. Liu, B. Q., Song, C., Sun, C., Zhou, S. G. & Zhu, J. Rhodium(III)-catalyzed indole synthesis using N–N bond as an internal oxidant. *J. Am. Chem. Soc.* **135**, 16625–16631 (2013).

34. Liu, G. X., Shen, Y. Y., Zhou, Z. & Lu, X. Y. Rhodium(III)-catalyzed redox-neutral coupling of N-phenoxyacetamides and alkynes with tunable selectivity. *Angew. Chem. Int. Ed.* **52**, 6033–6037 (2013).

35. Fukui, Y. et al. Tunable arylative cyclization of 1,6-enynes triggered by rhodium(III)-catalyzed C–H activation. *J. Am. Chem. Soc.* **136**, 15607–15614 (2014).

36. Jayakumar, J. et al. One-pot synthesis of highly substituted poly-heteroaromatic compounds by rhodium(III)-catalyzed multiple C–H activation and annulation. *Angew. Chem. Int. Ed.* **53**, 9889–9892 (2014).

37. Huang, H. W., Ji, X. C., Wu, W. Q. & Jiang, H. F. Transition metal-catalyzed C–H functionalization of N-oxyenamine internal oxidants. *Chem. Soc. Rev.* **44**, 1155–1171 (2015).

38. Geiger, W. E. Organometallic electrochemistry: Origins, development, and future. *Organometallics* **26**, 5738–5765 (2007).

39. Jutand, A. Contribution of electrochemistry to organometallic catalysis. *Chem. Rev.* **108**, 2300–2347 (2008).

40. Werlé, C. & Meyer, K. Organometallic electrochemistry: Redox catalysis going the smart way. *Organometallics* **38**, 1181–1185 (2019).

41. Siu, J. C., Fu, N. K. & Lin, S. Catalyzing electrosynthesis: A homogeneous electrocatalytic approach to reaction discovery. *Acc. Chem. Res.* **53**, 547–560 (2020).

42. Ma, C. et al. Recent advances in organic electrosynthesis employing transition metal complexes as electrocatalysts. *Sci. Bull.* **66**, 2412–2429 (2021).

43. Zhu, C. J., Ang, N. W. J., Meyer, T. H., Qiu, Y. A. & Ackermann, L. Organic electrochemistry: Molecular syntheses with potential. *Acs. Cent. Sci.* **7**, 415–431 (2021).

44. Cheng, X. et al. Recent applications of homogeneous catalysis in electrochemical organic synthesis. *CCS Chem.* **4**, 1120–1152 (2022).

45. Malapit, C. A. et al. Advances on the merger of electrochemistry and transition metal catalysis for organic synthesis. *Chem. Rev.* **122**, 3180–3218 (2022).

46. Fu, N. K., Sauer, G. S., Saha, A., Loo, A. & Lin, S. Metal-catalyzed electrochemical diazidation of alkenes. *Science* **357**, 575–579 (2017).

47. Yang, Q. L. et al. Palladium-catalyzed C(sp$^3$)—H oxygenation via electrochemical oxidation. *J. Am. Chem. Soc.* **139**, 3293–3298 (2017).

48. Gao, X. L., Wang, P., Zeng, L., Tang, S. & Lei, A. W. Cobalt(II)-catalyzed electrooxidative C–H amination of arenes with alkylamines. *J. Am. Chem. Soc.* **140**, 4195–4199 (2018).

49. Qiu, Y. A., Scheremetjew, A. & Ackermann, L. Electro-oxidative C–C alkenylation by rhodium(III) catalysis. *J. Am. Chem. Soc.* **141**, 2731–2738 (2019).

50. Wu, Z. J. et al. Scalable rhodium(III)-catalyzed Aryl C–H phosphorylation enabled by anodic oxidation induced reductive elimination. *Angew. Chem. Int. Ed.* **58**, 16770–16774 (2019).

51. Song, L. et al. Dual electrocatalysis enables enantioselective hydrocyanation of conjugated alkenes. *Nat. Chem.* **12**, 747–754 (2020).

52. Hamby, T. B., LaLama, M. J. & Sevov, C. S. Controlling Ni redox states by dynamic ligand exchange for electroreductive Csp3–Csp2 coupling. *Science* **376**, 410–416 (2022).

53. Zhang, B. X. et al. Ni-electrocatalytic Csp3–Csp3 doubly decarboxylative coupling. *Nature* **606**, 313–318 (2022).

54. Su, Z. M. et al. Ni- and Ni/Pd-Catalyzed reductive coupling of lignin-derived aromatics to access biobased plasticizers. *ACS Cent. Sci.* **9**, 159–165 (2023).

55. Ma, C., Fang, P. & Mei, T. S. Recent advances in C–H functionalization using electrochemical transition metal catalysis. *ACS Catal.* **8**, 7179–7189 (2015).

56. Ackermann, L. Metalla-electrocatalyzed C–H activation by earth-abundant 3d metals and beyond. *Acc. Chem. Res.* **53**, 84–104 (2020).

57. Jiao, K.-J. et al. Site-Selective C–H functionalization via synergistic use of electrochemistry and transition metal catalysis. *Acc. Chem. Res.* **53**, 300–310 (2020).

58. Qiu, Y. A., Zhu, C., Stangier, M., Struwe, J. & Ackermann, L. Rhodaelectro-catalyzed C–H and C–C activation. *CCS Chem.* **3**, 1529–1552 (2021).

59. Kumar, V., Maayuri, R., Mantry, L. & Gandeepan, P. Recent advances in rhodium-catalyzed electrochemical C–H activation. *Chem. Asian J.* **18**, e202300060 (2023).

60. Xu, F., Li, Y. J., Huang, C. & Xu, H. C. Ruthenium-catalyzed electrochemical dehydrogenative alkyne annulation. *ACS Catal.* **5**, 3820–3824 (2018).

61. Huang, Y. Q. et al. Electrochemical rhodium-catalyzed enantioselective C–H annulation with alkynes. *CCS Chem.* **4**, 3181–3189 (2022).

62. Qiu, Y. A. et al. Electrooxidative rhodium-catalyzed C–H/C–H activation: Electricity as oxidant for cross-dehydrogenative alkenylation. *Angew. Chem. Int. Ed.* **57**, 5828–5832 (2018).

63. Qiu, Y. A., Stangier, M., Meyer, T. H., Oliveira, J. C. A. & Ackermann, L. Iridium-catalyzed electrooxidative C–H activation by chemoselective redox-catalyst cooperation. *Angew. Chem. Int. Ed.* **57**, 14179–14183 (2018).

64. Choi, I., Messinis, A. M., Hou, X. Y. & Ackermann, L. A strategy for site- and chemoselective C–H alkenylation through osmaelectrooxidative catalysis. *Angew. Chem. Int. Ed.* **60**, 27005–27012 (2021).

65. Münchow, T. V., Dana, S., Xu, Y., Yuan, B. B. & Ackermann, L. Enantioselective electrochemical cobalt-catalyzedaryl C–H activation reactions. *Science* **379**, 1036–1042 (2023).

66. Mei, R. H., Sauermann, N., Oliveira, J. C. A. & Ackermann, L. Electroremovable traceless hydrazides for cobalt-catalyzed electro-oxidative C–H/N–H activation with internal alkynes. *J. Am. Chem. Soc.* **140**, 7913–7921 (2018).

67. Qiu, Y. A., Tian, C., Massignan, L., Rogge, T. & Ackermann, L. Electrooxidative ruthenium-catalyzed C–H/O–H annulation by weak O-coordination. *Angew. Chem. Int. Ed.* **57**, 5818–5822 (2018).

68. Tang, S., Wang, D., Liu, Y. C., Zeng, L. & Lei, A. W. Cobalt-catalyzed electrooxidative C-H/N-H [4+2] annulation with ethylene or ethyne. *Nat. Commun.* **9**, 798 (2018).

69. Yang, Q. L. et al. Electrochemistry-enabled Ir-catalyzed vinylic C–H functionalization. *J. Am. Chem. Soc.* **141**, 18970–18976 (2019).

70. Kong, W. J., Shen, Z. G., Finger, L. H. & Ackermann, L. Electrochemical access to Aza-polycyclic aromatic hydrocarbons: Rhoda-electrocatalyzed domino alkyne annulations. *Angew. Chem. Int. Ed.* **59**, 5551–5556 (2020).

71. Stangier, M., Messinis, A. M., Oliveira, J. C. A., Yu, H. & Ackermann, L. Rhodaelectro-catalyzed access to chromones via formyl C–H activation towards peptide electro-labeling. *Nat. Commun.* **12**, 4736 (2021).

72. Xing, Y. K. et al. Divergent rhodium-catalyzed electrochemical vinylic C–H annulation of acrylamides with alkynes. *Nat. Commun.* **12**, 930 (2021).

73. Xing, Y. K., Wang, Z. H., Fang, P., Ma, C. & Mei, T. S. Divergent synthesis of aryl amines and dihydroquinazolinones *via* electrochemistry-enabled rhodium-catalyzed C–H functionalization. *Sci. China Chem.* **66**, 2863–2870 (2023).

74. Wang, Y. L., Oliveira, J. C. A., Lin, Z. P. & Ackermann, L. Electro-oxidative rhodium-catalyzed [5+2] annulations via C-H/O-H activations. *Angew. Chem. Int. Ed.* **60**, 6419–6424 (2021).

75. Yuan, Y. M. et al. Scalable rhodaelectro-catalyzed expedient access to seven-membered Azepino[3,2,1-*hi*]indolesvia [5 + 2] C–H/N–H annulation. *CCS Chem.* **4**, 1858–1870 (2022).

76. Hoque, M. A., Gerken, J. B. & Stahl, S. S. Synthetic dioxygenase reactivity by pairing electrochemical oxygen reduction and water oxidation. *Science* **383**, 173–178 (2024).

77. Hoque, M. A., Jiang, T., Poole, D. L. & Stahl, S. S. Manganese-mediated electrochemical oxidation of thioethers to sulfoxides using water as the source of oxygen atoms. *J. Am. Chem. Soc.* **146**, 21960–21967 (2024).

78. Caron, S., Dugger, R. W., Ruggeri, S. G., Ragan, J. A. & Ripin, D. H. B. Large-scale oxidation in the pharmaceutical industry. *Chem. Rev.* **106**, 2943–2989 (2006).

79. Burns, N. Z., Baran, P. S. & Hoffmann, R. W. Redox economy in organic synthesis. *Angew. Chem. Int. Ed.* **48**, 2854–2867 (2009).

80. Wang, Y. H., Pegis, M. L. & Stahl, S. S. Molecular cobalt catalysts for $O_2$ reduction: Low-overpotential production of $H_2O_2$ and comparison with iron-based catalysts. *J. Am. Chem. Soc.* **139**, 16458–16461 (2017).

81. Wang, Y. H. et al. Kinetic and mechanistic characterization of low-overpotential, $H_2O_2$-selective reduction of $O_2$ catalyzed by $N_2O_2$-ligated cobalt complexes. *J. Am. Chem. Soc.* **140**, 10890–10899 (2018).

82. Stamoulis, A. G., Bruns, D. L. & Stahl, S. S. Optimizing the synthetic potential of $O_2$: Implications of overpotential in homogeneous aerobic oxidation catalysis. *J. Am. Chem. Soc.* **145**, 17515–17526 (2023).

83. Bauer, D. J. et al. 4′,6-Dichloroflavan (BW683C), a new anti-rhinovirus compound. *Nature* **292**, 369–370 (1981).

84. Nicolaou, K. C. et al. Natural product-like combinatorial libraries based on privileged structures. 1. general principles and solid-phase synthesis of benzopyrans. *J. Am. Chem. Soc.* **122**, 9939–9953 (2000).

85. Gumula, I. et al. Flemingins G–O, cytotoxic and antioxidant constituents of the leaves of Flemingia grahamiana. *J. Nat. Prod.* **77**, 2060–2067 (2014).

86. Pratap, R. & Ram, V. J. Natural and synthetic chromenes, fused chromenes, and versatility of dihydrobenzo[h]chromenes in organic synthesis. *Chem. Rev.* **114**, 10476–10526 (2014).

87. Lennox, A. J. J., Nutting, J. E. & Stahl, S. S. Selective electrochemical generation of benzylic radicals enabled by ferrocene-based electron-transfer mediators. *Chem. Sci.* **9**, 356–361 (2018).

88. Jung, K.-H., Müller, M. & Schmidt, R. R. Intramolecular O-glycoside bond formation. *Chem. Rev.* **100**, 4423–4442 (2000).

89. Yang, Y. & Yu, B. Recent advances in the chemical synthesis of C-glycosides. *Chem. Rev.* **117**, 12281–12356 (2017).

90. Walker, B. R., Manabe, S., Brusoe, A. T. & Sevov, C. S. Mediator-enabled electrocatalysis with ligandless copper for anaerobic Chan-Lam coupling reactions. *J. Am. Chem. Soc.* **143**, 6257–6265 (2021).

## Acknowledgements

## Author contributions

Y.-Q.H. and L.Z. designed and preformed the experiments. Y.-Q.H. and T.-S.M. directed the project. Y.-Q.H. and T.-S.M. revised the manuscript. Y.-Q.H. and T.-S.M. wrote the manuscript with input from all authors. All authors analyzed the results and commented on the manuscript.

## Competing interests

The authors declare no competing interests.

## Additional information

**Supplementary information** The online version contains supplementary material available at https://doi.org/10.1038/s41467-025-59405-x.

**Correspondence** and requests for materials should be addressed to Tian-Sheng Mei.

**Peer review information** *Nature Communications* thanks the anonymous reviewer(s) for their contribution to the peer review of this work. A peer review file is available.

**Reprints and permissions information** is available at http://www.nature.com/reprints

**Publisher's note** Springer Nature remains neutral with regard to jurisdictional claims in published maps and institutional affiliations.